Simulated Muscle Fiber

Documentation Date: July 2024

History:

- The initial model was developed by Cannon, to simulate the consequences for sodium channel gain-of-function defects on the susceptibility to myotonia and periodic paralysis (Cannon, Brown et al. 1993).

  Two-compartment model, Sarcolemma (Sarc) and Transverse Tubule (TT), coupled by an access resistance, R_a.

  The geometric relation between the Sarc and TT was set by a single parameter, the ratio of TT to Sarc membrane surface area $\gamma = 4.8$ (Adrian, Costantin et al. 1969). This initial version had no explicit dependence on fiber radius. Channel density in the TT membrane was adjustable by using a scaling factor of η_x, the TT/Sarc density ratio.

  Ion channels: NaV, Kdr, Leak.

  No Kir, ClC-1

  Open channel conductances were Ohmic (linear). The leak conductance was non-selective, with a reversal potential set by the GHK voltage equation with $P_{Na}/P_K = 0.01$. In this way, V_{rest} was influence by $[K^+]_{out}$. Because P_{open} for Kdr was so low for $V < -55\ mV$, the delayed rectifier had essentially no impact on V_{rest}.

  Pumps: none

  Cotransporters: none

- Model evolution.
  Over the next 30 years (1993 – 2023), we incrementally modified the model to include additional features that were subsequently learned to have a large impact on setting and stabilizing V_{rest} in the context of ion channelopathies that cause periodic paralysis. Major changes included:

  - Membrane Compartments. The ratio of TT to Sarc surfaced area now depends on fiber radius. We continue to use a lumped, single compartment for the TT, rather than concentric shells, because a single compartment emulates all the major features of use-dependent ion accumulation that drives myotonic after-discharges. The model simulates short mammalian fibers (length < 500 μm), wherein the fiber is effectively space-clamped with no length dependence for the Sarc or TT membrane potentials.

  - Ion channels.
    NaV (with slow and fast inactivation), Kir, Kdr, KCNQ, ClC-1. The open channel

IV relation is determined by the GHK current equation (i.e. not linear or Ohmic). A gating pore leak conductance is included to simulate the aberrant current conducted by mutant channels in HypoPP.

Channels not included: KATP, MaxiK, CaV, stretch, or leak

- Pumps.
  Na,K-ATPase is simulated as two isoforms:
  - $\alpha 1$ high affinity for external K, primarily in the sarcolemma
  - $\alpha 2$ low affinity for external K, primarily in the T-tubule

- Transporters.
  NKCC1 is present in the Sarc and TT. The chemical potential (no V-dep) normally favors influx, and this is the major mechanism by which intracellular $[Cl^-]$ is higher than the passive equilibrium value that would otherwise be determined by electrodiffusion through ClC-1 channels with the steady-state balance determined by V_{rest}.

2024 Model:

- Membrane compartments.
  - Sarcolemma.
  - Transverse tubule. Single, lumped compartment coupled to the sarcolemma by an access resistance, R_a.

    In the single, lumped-compartment model, the ratio of TT_SA to Sarc_SA is (Peachey 1965):

$$\gamma = \left(\frac{2}{r}\right)\left(\frac{\rho}{\varsigma}\right)$$

    where,

$$r = fiber\ radius\ (cm)$$
$$\rho = TT\ volume\ per\ fiber\ volume = 0.003$$
$$\varsigma = TT\ volume\ to\ surface\ area = 1.25\ x\ 10^{-6}\ cm$$

The computational analysis for this two-compartment model of a muscle fiber is governed by a pair of coupled equations (Cannon, Brown et al. 1993):

$$I_m = C_m \frac{dV_{sarc}}{dt} + \sum I_{ionic\_sarc} + \frac{V_{sarc} - V_{TT}}{R_a} \quad \text{(eqn. 1)}$$

$$\frac{V_{sarc} - V_{TT}}{R_a} = \gamma \left[C_m \frac{dV_{TT}}{dt} + \sum I_{ionic\_TT} \right] \quad \text{(eqn. 2)}$$

I_m	Total current from the myoplasm to the extracellular space (mA/cm^2), which is a combination of the capacitive, ionic (via the sarcolemma) and TT currents.
I_{ionic_sarc}	Ionic currents across the sarcolemma, per unit area of sarc (mA/cm^2), conducted by ion channels and pumps.
I_{ionic_TT}	Ionic currents across the transverse tubules, per unit area of TT (mA/cm^2), conducted by ion channels and pumps.
V_{sarc}, V_{TT}	Membrane potential for the sarc and the TT (mV).
R_a	Access resistance from the TT to extracellular space, (Ω-cm^2).
C_m	Membrane specific capacitance (mF/cm^2).
γ	Ratio of TT surface area per unit surface area of the sarc.

Solutions to eqns. 1 & 2 are computed by Euler integration with an adaptive dt step size such that $dV_{sarc} < 0.05$ mV.

- Ion Channels.

The open channel IV relation for all channels (Na, K, Cl, gating pore) is simulated using the constant field current equation (GHK). For permeant ion x,

$$I_{X\_open}(V) = P_x z_x^2 \frac{VF^2}{RT} \frac{[x]_i - [x]_o \exp(-z_x FV/RT)}{1 - \exp(-z_x FV/RT)}$$

Individual currents are computed as the probability of being open, $P_{open_x}(V,t)$, times the open channel IV. In general:

$$I_X(V,t) = P_{open_x}(V,t) I_{x\_open}(V)$$

Sodium Channel:

The model includes the possibility for two populations of sodium channels, with independent gating properties, to simulate the co-expression of WT and mutant channels. Both populations of sodium channels are simulated by the same HH type model (Hodgkin and Huxley 1952):

$$I_{Na} = m^3 s[h(1-f) + f] I_{Na\_open}(V)$$

$m(V,t)$	activation (Hodgkin-Huxley model)
$h(V,t)$	fast inactivation (Hodgkin-Huxley model)
$s(V,t)$	slow inactivation (extension to Hodgkin-Huxley model)
f	fraction of Na channels that does NOT fast inactivate; “persistent”

Fast inactivation: $\frac{dh}{dt} = \alpha(1-h) - \beta h$;

$\alpha(V)$ voltage-dependent rate of recovery
$\beta(V)$ voltage-dependent rate of inactivating

Steady-State: $h_\infty(V) = \frac{\alpha}{\alpha+\beta}$

For parameter selection of V_h and k_h, our experimental data from the measurement of steady-state (fast) inactivation are fit to:

$$h_\infty(V) = \frac{1}{1+\exp\left(\frac{V-V_h}{k_h}\right)}$$

Kinetics: $\tau_h(V) = \frac{1}{\alpha(V)+\beta(V)}$

Parameter selection is based on fitting our experimentally determined kinetics of "entry to" and "recovery from" fast inactivation using the traditional HH rate equations:

$$\alpha(V) = \frac{\alpha_h}{1+e^{(V-V_{\alpha h})/k_{\alpha h}}};\ \beta(V) = \frac{\beta_h}{1+e^{-(V-V_{\beta h})/k_{\beta h}}}$$

Finally, these fitted functions for $h_\infty(V)$ and $\tau_h(V)$ are then converted back to the effective HH rate constants as:

$$\alpha_{eff}(V) = h_\infty(V)/\tau_h(V); \quad \beta_{eff}(V) = (1-h(V))/\tau_h(V)$$

Slow Inactivation:

A similar process is used for the slow-inactivation state variable, s, except the steady-state voltage dependence has a non-zero "pedestal" of amplitude s_0 as V becomes more positive (Hayward, Brown et al. 1997).

$$s_\infty(V) = s_0 + \frac{1-s_0}{1+\exp\left(\frac{V-V_s}{k_s}\right)}$$

Activation: $\frac{dm}{dt} = \alpha(1-m) - \beta m$;

$\alpha(V)$ voltage-dependent rate of activating
$\beta(V)$ voltage-dependent rate of deactivating

Steady-State: $m_\infty(V) = \frac{\alpha}{\alpha+\beta}$

For parameter selection of V_m and k_m, our experimental data for the relative peak conductance, $G(V)$, are fit to:

$$m_\infty^3(V) = G(V) = \frac{1}{1+\exp\left(\frac{V-V_m}{k_m}\right)}$$

Kinetics: $\tau_m(V) = \frac{1}{\alpha(V)+\beta(V)}$

Parameter selection is based on fitting our experimentally determined kinetics of activation and deactivation using the traditional HH rate equations:

$$\alpha(V) = \frac{\alpha_m(V-V_{\alpha m})}{1+e^{(V-V_{\alpha m})/k_{\alpha m}}};\ \beta(V) = \beta_m e^{-(V-V_{\beta m})/k_{\beta m}}$$

Finally, the fitted function for $m_\infty(V)$ and $\tau_m(V)$ are then converted back to the effective HH rate constants as:

$$\alpha_{eff}(V) = m_\infty(V)/\tau_m(V); \quad \beta_{eff}(V) = (1-m(V))/\tau_m(V)$$

Potassium Channels:

Inward Rectifier (Kir2.x type).

This simulated channel has “strong” rectification, like the Kir2.x subfamily of channels. $I_{Kir}(V)$ is essentially instantaneous, with no dependence on time in the model (Hagiwara and Takahashi 1974).

$I_{Kir} = r(V,[K])I_{K\_open}(V)$, where

$r(V,[K])$ is a rectification term (i.e. P_{open}).

$$r(V,[K]) = \left[1+e^{(V-E_K-V_{IR})/v}\right]^{-1}$$

Notice the $[K]$ dependence, via E_K. This is required because the voltage at which rectification occurs depends on the K gradient.

A-type Delayed Rectifier.

The predominant voltage-activated K^+ channel in mammalian skeletal muscle is a “delayed rectifier” that slowly inactivates on a time scale of about 200 msec (DiFranco, Quinonez et al. 2012). Many models of the muscle fiber do not include inactivation for the simulated delayed-rectifier conductance because they were based on voltage-clamp data over a short time scale (< 100 msec), during which inactivation is minimal.

$I_{Kdr} = n^4 p I_{K\_open}(V)$

$n(V,t)$ is the standard H-H Model activation term.

$p(V,t)$ is an inactivation term, like h for Na channels.

KCNQ (Kv7.x type).

KCNQ type K^+ channels are included in the model fiber to simulate the effects of KCNQ channel openers such as retigabine (Quinonez, DiFranco et al. 2023).

$$I_{KCNQ} = qI_{K\_open}(V)$$

$q(V,t)$ is the activation state variable.

$$\frac{dq}{dt} = \alpha(1-q) - \beta q$$

$$\alpha(V) = \alpha_q e^{-(V-V_{\alpha q})/k_{\alpha q}} \;;\; \beta(V) = \beta_q e^{-(V-V_{\beta q})/k_{\beta q}}$$

Chloride Channel:

The simulated ClC-1 channel uses a modified open channel IV relation that includes a membrane surface charge ($V' =$ -120 mV). The effect is to reduces extracellular [Cl^-] locally at the membrane surface, to account for the experimental observation that the open-channel IV had mild inward rectification rather than the outward rectification predicted from the [Cl^-] gradient of the bulk solution (DiFranco, Herrera et al. 2011). This surface charge term changes the curvature of the IV relation but not the reversal potential.

$$I_{Cl\_open} = \frac{P_{Cl}(V-V')F^2}{RT} \; \frac{[Cl]_o e^{V'F/RT} - [Cl]_i e^{-(V-V')F/RT}}{1-e^{-(V-V')F/RT}}$$

$$I_{Cl} = cI_{Cl\_open}(V)$$

$c(V,t)$ is the ClC-1 channel activation term.

$$\frac{dc}{dt} = \alpha(1-c) - \beta c$$

$$\alpha(V) = \frac{\alpha_c}{1+e^{(V-V_{\alpha c})/k_{\alpha c}}}; \quad \beta(V) = \frac{\beta_c}{1+e^{-(V-V_{\beta c})/k_{\beta c}}}$$

nAChR Channel:

To simulate synaptic activation of the fiber at the NMJ, the model includes a non-selective cation channel ($P_K/P_{Na} \sim 1.1$) for which channel activation is modeled as an all-or-none transition from closed to open for a specified duration (typically 0.5 msec).

- Pumps.

  The Na,K-ATPase pump is electrogenic, with 3 Na^+ ions leaving and 2 K^+ ions entering the fiber with each cycle, and therefore has a modest voltage-dependence, $f(V)$, favored when V is more positive. The pump turn-over rate is dependent on $[Na]_i$ and $[K]_o$ (Wallinga, Meijer et al. 1999).

$$I_{Na,K} = \frac{Ff(V)J_{Na,K}}{(1 + K_{mK}/[K]_O)^2 (1 + K_{mNa}/[Na]_i)^3}$$

$$f(V) = 1/(1 + 0.12e^{-0.1\,VF/RT} + 0.04\sigma e^{-VF/RT})$$

$$\sigma(Na) = \frac{1}{7}\left(e^{[Na]_O/67.3} - 1\right)$$

  The fiber contains two different isoforms: α_1 with high K affinity on the Sarc, α_2 with low K affinity primarily in the TT (DiFranco, Hakimjavadi et al. 2015).

- Transporters.

  The NKCC1 co-transporter is electroneutral, with no net charge transfer or ionic current. This transporter makes important contributions to fiber excitability, however, by setting the transmembrane ion gradients for Cl^- and Na^+ via the large influence on $[Cl]_i$ and $[Na]_i$.

  The electroneutral flux via NKCC1 is computed as (Gallaher, Bier et al. 2009),

$$J^x_{NKCC} = \beta_x J_0 \left[log\left(\frac{[Na]_O}{[Na]_i}\right) + log\left(\frac{[K]_O}{[K]_i}\right) + 2log\left(\frac{[Cl]_O}{[Cl]_i}\right)\right]$$

  where for $x \in \{Na, K, Cl\}$, $\beta_x = 1$ for Na and K; $\beta_x = 2$ for Cl.

- Flux (current) – dependent ion gradients.

  The net current (plus flux from the cotransporter) for each species of ion is used to calculate the change in $[ion]$ for the TT compartment or for the intracellular myoplasm. Ion concentrations are fixed for the extracellular space, to simulate the case of an isolated fiber in an experimental recording chamber (effectively, infinite extracellular volume). Equilibration of $[ion]$ between the TT and extracellular space is simulated as a first-order passive diffusion process for the concentration gradient, with a time constant of $\tau_{diff} =$ 350 msec.

  For example, the change for $[K]_{TT}$ is computed as (Cannon, Brown et al. 1993):

$$\frac{d[K]_{TT}}{dt} = \frac{I_{Kir\_TT} + I_{Kdr\_TT} + I_{KCNQ\_TT} - J^K_{NKCC\_TT} - 2I_{pump\_TT}}{F\varsigma} - \frac{[K]_{TT} - [K]_O}{\tau_{diff}}$$

Computational Method:

Simulations to compute the response of the model fiber are performed in the Windows operating environment, in custom code written in FreeBASIC (https://www.freebasic.net/). The code is compiled and runs as a stand-alone application with a graphical user interface (Muscle_Sim_Vxxx.exe). Model parameters are defined by an input file (MS Excel format) and the results are available as bit-mapped images of graphic displays or as numerical values in CSV format.

Initial conditions $\{[ions], V_{sarc}, V_{TT}\}$ may either be pre-set or determined automatically by searching for steady-state solutions where the net flux for all ions and dV/dt are simultaneously 0. The differential equations for membrane potentials (Eqn 1 & 2, above) and for the state variables that determine channel gating were solved by numerical integration (Euler) with an adaptive step size $dt_{min} < dt < dt_{max}$, with the constraint that for any single step $dV < 0.05$ mV.

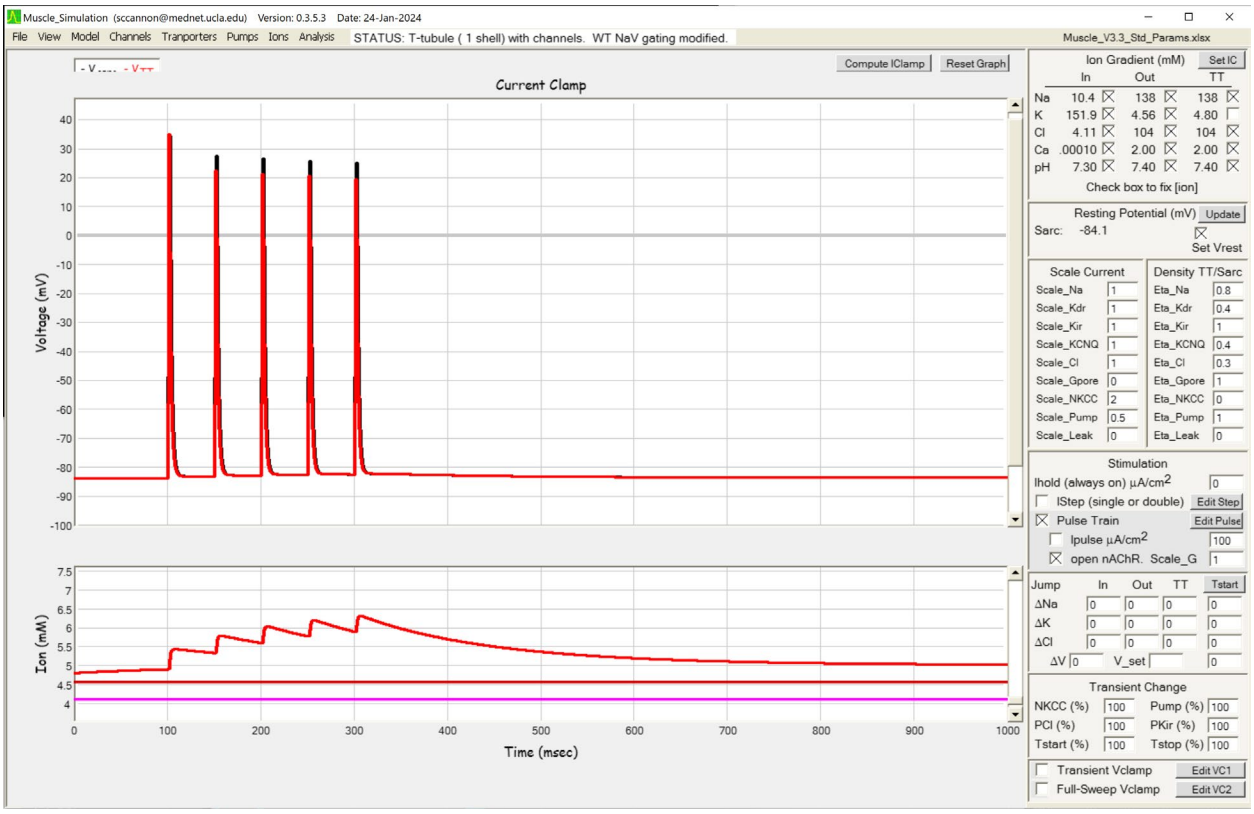

Figure 1. Example results from a simulation with muscle_sim_V3.5, wherein the fiber was stimulated by nAChR activation at 20 Hz for 5 pulses. The use-dependent change in $[K^+]_{TT}$ is shown in the lower panel.

Literature Cited.

Adrian, R. H., L. L. Costantin and L. D. Peachey (1969). "Radial spread of contraction in frog muscle fibres." J Physiol **204**(1): 231-257.

Cannon, S. C., R. H. Brown, Jr. and D. P. Corey (1993). "Theoretical reconstruction of myotonia and paralysis caused by incomplete inactivation of sodium channels." Biophys J **65**(1): 270-288.

DiFranco, M., H. Hakimjavadi, J. B. Lingrel and J. A. Heiny (2015). "Na,K-ATPase alpha2 activity in mammalian skeletal muscle T-tubules is acutely stimulated by extracellular K+." J Gen Physiol **146**(4): 281-294.

DiFranco, M., A. Herrera and J. L. Vergara (2011). "Chloride currents from the transverse tubular system in adult mammalian skeletal muscle fibers." J Gen Physiol **137**(1): 21-41.

DiFranco, M., M. Quinonez and J. L. Vergara (2012). "The delayed rectifier potassium conductance in the sarcolemma and the transverse tubular system membranes of mammalian skeletal muscle fibers." J Gen Physiol **140**(2): 109-137.

Gallaher, J., M. Bier and J. Siegenbeek van Heukelom (2009). "The role of chloride transport in the control of the membrane potential in skeletal muscle--theory and experiment." Biophys Chem **143**(1-2): 18-25.

Hagiwara, S. and K. Takahashi (1974). "The anomalous rectification and cation selectivity of the membrane of a starfish egg cell." J Membr Biol **18**(1): 61-80.

Hayward, L. J., R. H. Brown, Jr. and S. C. Cannon (1997). "Slow inactivation differs among mutant Na channels associated with myotonia and periodic paralysis." Biophysical Journal **72**: 1204-1219.

Hodgkin, A. L. and A. F. Huxley (1952). "A quantitative description of membrane current and its application to conduction and excitation in nerve." Journal of Physiology **117**: 500-544.

Peachey, L. D. (1965). "The sarcoplasmic reticulum and transverse tubules of the frog's sartorius." The Journal of cell biology **25**(3): Suppl:209-231.

Quinonez, M., M. DiFranco, F. Wu and S. C. Cannon (2023). "Retigabine suppresses loss of force in mouse models of hypokalaemic periodic paralysis." Brain **146**(4): 1554-1560.

Wallinga, W., S. L. Meijer, M. J. Alberink, M. Vliek, E. D. Wienk and D. L. Ypey (1999). "Modelling action potentials and membrane currents of mammalian skeletal muscle fibres in coherence with potassium concentration changes in the T-tubular system." Eur Biophys J **28**(4): 317-329.